

LOG ANALYSIS IN LOW-PERMEABILITY GAS SAND SEQUENCES
- CORRECTING FOR VARIABLE UNFLUSHED GAS SATURATION

Gerald C. Kukul
CER Corporation, Las Vegas

ABSTRACT

This paper outlines the technology required to correct porosity for variable unflushed gas saturation. Gas effect on density and neutron logs is fundamental to gas detection. However, in mud drilled wells, a mud filtrate invasion front generally advances radially from the borehole wall and displaces gas within a "flushed zone." Peripheral to the flushed zone is an "invaded zone" characterized by less thorough gas displacement and, therefore, a higher residual gas saturation. Since density and neutron tools have depths of investigation which are somewhat shallow, gas effect is significantly influenced by the depth of invasion and the thoroughness of flushing.

The depth of invasion is generally shallow in high porosity reservoirs and deep in lower porosities. Data presented within this paper, however, show that this generally accepted logging axiom is true only up to a certain point. When low porosity tight gas sand reservoirs are at a critical minimum water permeability, no invasion takes place. Above this minimum permeability, both time and differential pressure control invasion profile. The consequence of this phenomenon is that the porosity of a very poor quality gas reservoir is overestimated, water saturation is underestimated, and the producible gas zone does not contrast well with the tight zone. Thus, the goal of log analysis - to discern the better zones for completion is not achieved.

An iterative mathematical model, involving the density, neutron, and gamma ray response equations, is developed to solve for " S_{X0} " which in this case is actually the average saturation of the zone investigated by the density and neutron tools. This " S_{X0} " is then used to provide more reliable porosity interpretation. This technique is verified by comparing log calculations to core data.

Aside from more reliable porosity, interesting spinoffs of the technique are: 1) a more reliable procedure to interpret gas saturation in uninvaded formations (independent of R_w and R_t); 2) a new procedure to interpret R_w in uninvaded formations; and 3) a new system to identify invaded and, hence, producible gas zones.

INTRODUCTION

Existing logging techniques and interpretation methods developed for high porosity - good quality reservoirs must often be modified when evaluating low porosity - low permeability "tight" sands.

The logging problems characteristic of the tight gas sands (TGS) resource were discussed generally by Kukal et al (1983). They determined that water saturation is the most critical reservoir parameter controlling sustained gas production. Accurate porosity analysis is critical to accurate saturation analysis - especially so in TGS where a 2 porosity unit (p.u.) error results in a 15 saturation unit error.¹

Kukal (1981) pointed out that failure to adequately correct for variable unflushed gas saturation in the density porosity equation typically results in a 2-4 p.u. error when analyzing porosity in gas sands having 8-12% porosity.²

Gas effect is normally compensated for in porosity calculations by: 1) assuming a constant flushed zone saturation (S_{X0}); 2) assuming that matrix corrected neutron and density porosities would read the same value with no gas effect and then solving for variable S_{X0} ; or 3) averaging the two porosities. The first method is an oversimplification and suffers when S_{X0} is variable. Techniques two and three are unsatisfactory when S_{X0} is variable and when clay influences the neutron response more than the density response.

Other techniques which treat S_{X0} as variable such as those proposed by Patchett and Coalson (1982) may be good approximations for S_{X0} when a formation is flushed.³ However, low permeability invasion studies performed by Sattler (1983) show that differential pressure, time, and permeability each exert strong influence on flushing kinetics.⁴ Data presented within this paper, in fact, suggest that TGS are essentially uninvaded under conditions of normal differential pressure operations, i.e., when the hydrostatic pressure of the mud column is in balance with formation pressure.

This paper presents a log analysis model to solve the problem of variable unflushed gas saturation. The "Kukal approach" or "Kukal equation" is outlined mathematically. This technique combines the neutron and density response equations and an independent clay indicator such as the gamma ray to solve for " S_{X0} " and porosity. The " S_{X0} " is actually the average water saturation of the zone investigated by the density and neutron tools. In unflushed gas formations, the saturation derived for the density-neutron zone (S_{dn}) could provide more reliable water saturations than those using conventional resistivity - porosity relations.

The approach provides more reliable porosities than methods relying solely on the density log or those which simply average neutron and density porosities. Since the S_{dn} is independent of resistivity (R_t) and formation water resistivity (R_w), the new saturation technique (S_{dn}) has application for the determination of R_w in unflushed gas saturated formations. Comparisons of near zone saturations (density-neutron) with far zone saturations (R_t) permit interpretation of invaded and hence permeable reservoirs. The technique also has application in other shallow-invasion type borehole environments, e.g., air-gas drilled holes and wells drilled with under-balanced pressure differentials.

CER Corporation has developed the "Kukal approach" into a new computer log interpretation system as described elsewhere (Kukal, 1983).⁵ This model has

been applied to TGS sequences in Texas (Cotton Valley), New Mexico (San Juan Basin), Colorado (Piceance Basin), Wyoming (Green River Basin) and Utah (Uinta Basin) and promises to be a powerful new procedure for the analysis of TGS.

DEPTH OF INVESTIGATION - DENSITY AND NEUTRON TOOLS

The depths of investigation of the various radioactivity porosity tools were measured experimentally by Sherman and Locke (1975).⁶ Two observations from that study are pertinent to this paper:

1. Depths of investigation of radioactivity porosity tools are generally shallow (4-12 inches) relative to the deep investigation of the resistivity tools (several feet).
2. Neutron tools read deeper than density tools in low porosity rocks.

When a formation is totally uninvaded, $S_{dn} = S_w$. With deep flushing, $S_{dn} = S_{xo}$. Since S_{dn} is defined as the average water saturation of the zone investigated by the density and neutron logs, the concept of this term may become confused when flushing is intermediate in depth, i.e., when the flushing radius is generally beyond the reading of the density and shallower than the major volume investigated by the neutron tool. Interestingly enough, however, the new approach is applicable throughout all invasion depths. This is borne out by log-core porosity comparisons and by the generally realistic saturations computed (S_{dn}).

EVIDENCE FOR VARIABLE AND GENERALLY SHALLOW INVASION IN TGS

Depth of invasion and thoroughness of flushing are generally quite variable in TGS. This is evidenced by log-core porosity crossplots, staged or overlap logging with different mud weights - at different points in time, and capillary pressure - relative permeability studies.

Log-core crossplots for cored intervals in TGS sequences typically demonstrate a gas effect upon the density log. Figure 1 (after Kukul, 1981)² is a composite of zone data from four TGS cored wells in western Wyoming. Calculated density porosity is crossplotted with core porosity. Grain density is measured and fluid density is assumed to be 1.0. The crossplot shows a rough 1:1 correlation for very low porosity values (0 - .06). Higher porosity values (.12 - .15) also appear to be crossplotting near unity. Low to moderate porosities in the .06 - .12 range show the greatest divergence between density porosity and core porosity.

A logical interpretation of these observations is that high gas saturations remain unflushed in the formation and are influencing the density tool response. The tool reads a lower bulk density than if the porosity is water

filled. The assumption of too high a fluid density causes porosity to be overestimated.

A line of 0.5 gas saturation is constructed for better visual analysis of Figure 1. Salient interpretations of this crossplot are as follows:

1. there are many points that fall between the $S_{XO} = 1.0$ and " S_{XO} " = 0.5 lines and some points that fall beyond the " S_{XO} " = 0.5 line, i.e., residual gas appears to be variable and could be dependent upon differential pressure, formation permeability, and time between penetration and logging;
2. low porosities tend to be associated with high irreducible water saturations -- this would cause very low (0 - .06) porosities to plot near the $S_{XO} = 1.0$ lines;
3. higher (.12 - .15) porosities tend to return to the $S_{XO} = 1.0$ line. This implies that higher porosities have a higher degree of flushing;
4. some formations of interest (especially those showing considerable crossover) may be uninvaded. This is evident because calculated " S_{XO} " is much lower than is anticipated in a flushed interval. " S_{XO} " approximates S_w .

Staged Logging of the CER MWX-2 well in the Rulison Gas Field, Piceance Basin, Colorado illustrates that flushing thoroughness is variable in TGS. Figure 2 is a composite of three log runs for the density (FDC) and compensated thermal neutron log (CNTA). The well was drilled in an area of considerable overpressuring, so it was necessary to increase mud weight throughout the drilling. The three log runs are keyed by:

1. solid curves (run 1 - 8.4 lb/gal mud - logged at TD of 5450');;
2. dashed curves (Run 2 - 11.0 lb/gal mud - logged two weeks later at a TD of 6700'); and
3. dotted curves (Run 3 - 14.7 lb/gal mud - logged six weeks after Run 1 at a TD of 8300').

It is an obvious interpretation from Figure 2 that there is a progressive decrease in gas effect on both the neutron and density curves with each successive log run. Invasion is thus dependent upon time and/or differential pressure. It is conceivable that some sands are totally uninvaded at the time of logging while others are rather thoroughly flushed. Simply relating S_{XO} to S_w or porosity is clearly not the answer to accurate fluid density estimation in formations that are not flushed.

Relative permeability curves constructed for individual TGS core samples, such as those presented by Thomas and Ward (1972)⁷ support the observation that water permeabilities of typical TGS are very low when water saturation is at or near irreducible.

High capillary pressures in these rocks either prohibit invasion or make the invasion phenomenon unobservable in normal time between penetration and logging. Reservoirs having such high capillary pressures are generally not productive. These uninvaded poor quality reservoirs do not contrast well with the better quality invaded sands. Porosity and gas saturation are overestimated. Thus, the goal of log analysis - to discern the paying intervals for completion is not achieved.

MODEL FOR CALCULATION OF VARIABLE GAS EFFECTS

An iterative mathematical model suitable for routine computer log analysis is developed to provide an effective interpretation of porosity in gas reservoirs having variable unflushed gas saturation. The model makes use of logs generally available - a density log, a neutron log (calibrated in porosity units) and a clay indicator log such as the gamma ray. No other logs are needed for porosity, however, a resistivity log is critical for reliable estimates of gas saturation in flushed formations, oil saturation, and permeability interpretations. A photo-electric effect measurement may be useful for matrix refinement.

The density and neutron response equations are the basis for the model. Each response equation is solved for porosity, the equations are set equal to each other, and then solved for "S_{xo}" - which is actually the average saturation in the zone investigated by the density and neutron tools. Since the clay content fraction remains an unknown, clay volume (V_{c1}) must be solved using an independent equation. When "S_{xo}" is computed, either porosity equation may be used to solve for gas corrected porosity.

Density response equation. The density tool responds to matrix, water, and hydrocarbon. The response equation is defined as:

$$\rho_b = \rho_{ma} - \rho_{ma} \phi + \phi [(1-S_{xo}) \rho_h + S_{xo} \rho_{mf}] \dots \dots \dots (1)$$

- where; ρ_b = bulk density, borehole corrected, g/cc
- ρ_{ma} = matrix density; matrix is the solid portion of the rock and excludes adsorbed water; in this sense, matrix density = grain density measurements of dried core; it includes framework minerals such as quartz and feldspar, clay minerals, and solid organic matter, g/cc
- ϕ = total porosity, including the volume occupied by adsorbed water, fraction of bulk volume
- S_{xo} = water saturation of the zone investigated by the density tool, fraction of pore volume
- ρ_h = hydrocarbon density, g/cc
- ρ_{mf} = density of water or mud filtrate in the zone investigated by the density tool, g/cc.

This equation treats the definition of matrix and perhaps porosity differently from other published equations, however, it makes sense to deal with solid matter in the rock as being matrix and with liquid adsorbed water as being water filled porosity.

Neutron response equation. The neutron tool responds to matrix, clay, water, and hydrocarbons and is defined as follows:

$$\phi_n = \phi [S_{x0} (\phi_n)_{mf} + (1-S_{x0})(\phi_n)_h] + V_{cl} (\phi_n)_{cl} - (\Delta\phi_n)_{ex} \dots (2)$$

- where; ϕ_n = neutron response when calibrated on the proper matrix and corrected for temperature and pressure effects
- ϕ = total porosity, fraction of bulk volume
- S_{x0} = water saturation of the zone investigated by the neutron tool, fraction of pore volume
- $(\phi_n)_{mf}$ = neutron response to water in the zone investigated by the neutron log
- $(\phi_n)_h$ = neutron response to formation hydrocarbon
- V_{cl} = clay content fraction of bulk volume
- $(\phi_n)_{cl}$ = neutron response to formation clay
- $(\Delta\phi_n)_{ex}$ = excavation effect neutron

Combined density and neutron response equations - the "Kukal equation." Each response equation is solved for porosity. Porosity is then eliminated by setting the two equations equal to each other. This equation is then solved for "S_{x0}" or more properly S_{Dn}. The algebra is as follows:

$$\phi = \frac{\rho_b - \rho_{ma}}{S_{x0} \rho_{mf} + (1-S_{x0}) \rho_h - \rho_{ma}} \dots (3)$$

$$\phi = \frac{\phi_n - V_{cl} (\phi_n)_{cl} + (\Delta\phi_n)_{ex}}{S_{x0} (\phi_n)_{mf} + (1-S_{x0})(\phi_n)_h} \dots (4)$$

$$\frac{\rho_b - \rho_{ma}}{S_{x0} \rho_{mf} + (1-S_{x0}) \rho_h - \rho_{ma}} = \frac{\phi_n - V_{cl} (\phi_n)_{cl} + (\Delta\phi_n)_{ex}}{S_{x0} (\phi_n)_{mf} + (1-S_{x0})(\phi_n)_h} \dots (5)$$

$$"S_{x0}" = \frac{(\phi_n)_h(\rho_b - \rho_{ma}) - (\rho_h - \rho_{ma})[\phi_n - V_{cl}(\phi_n)_{cl} + (\Delta\phi_n)_{ex}]}{(\rho_{mf} - \rho_h)[\phi_n - V_{cl}(\phi_n)_{cl} + (\Delta\phi_n)_{ex}] - [(\phi_n)_{mf} - (\phi_n)_h](\rho_b - \rho_{ma})} \dots (6)$$

where; "S_{x0}" = S_{dn} = the average water saturation of the zone investigated by the density and neutron tools, fraction of pore volume and all other terms were previously defined.

Equations and/or techniques to refine each parameter are given by Segesman and Liu (1971)⁸, Kukul (1981)², Kukul (1983)⁵, and Kukul and Hill (1983).⁹

An independent clay equation from the gamma ray. Since the clay content fraction remains an unknown, an independent clay equation from the gamma ray is utilized:

$$V_{cl} = \frac{GR - GR_{min}}{GR_{clay} - GR_{min}} \dots (7)$$

where; $GR_{clay} = \frac{GR_{max} - (1 - V_{clk})GR_{min}}{V_{clk}} \dots (8)$

- GR = gamma ray reading from log, API units
- GR_{min} = gamma ray response to a clean sand, API units
- GR_{clay} = gamma ray response to "pure clay," API units
- GR_{max} = gamma ray response to typical shale, API units
- V_{clk} = clay constant = fraction of clay present in a typical shale, fraction of matrix volume

The rationale for this new equation is discussed by Kukul and Hill (1983).⁹

Porosity Calculation. One or more "S_{x0}" iterations are required since there is an S_{x0} term in the excavation effect equation. Porosity is then calculated using equations 3 or 4.

Using the "Kukul equation" for clay volume calculations. Matrix parameter refinement is facilitated by using equation 5 as a clay equation. This is done by making "S_{x0}" constant (for example totally flushed) and solving for V_{cl}:

$$(V_{cl})_{dn} = \frac{\phi_n + (\Delta\phi_n)_{ex} - (\rho_b - \rho_{ma}) [S_{xo} (\phi_n)_{mf} + (1-S_{xo}) (\phi_n)_h]}{S_{xo} \rho_{mf} + (1-S_{xo}) \rho_h - \rho_{ma}} \cdot \cdot \cdot (9)$$

$$(\phi_n)_{cl}$$

Figure 3 is a trace plot of foot-by-foot solutions of equation 9 (clay volume from the density-neutron) and equation 7 (clay volume from the gamma ray). The interval plotted is the Cozzette Sandstone, CER MWX-1 well. Figure 4 is the same plot for the Corcoran Sandstone. Parameters are refined properly when the "clayplot" gives similar results for both equations. The upper bound calibration point is the clay constant $(V_{cl}k)$ which in this case is 0.60. The lower bound verification point is zero V_{cl} . It should be noted that $(V_{cl})_{dn}$ may calculate lower than $(V_{cl})_{gr}$ in a gas zone with an " S_{xo} " less than 1.0. Calculated $(V_{cl})_{dn}$ is frequently less than zero in clean uninvaded gas sands - because of the erroneous assumption that " S_{xo} " = 1.0. Cozzette Sandstones (Figure 3) are interpreted to be generally flushed at time of logging whereas the Corcoran Sandstones (Figure 4) appear to be totally uninvaded.

The "Clayplot" indicates that both the gamma ray and the neutron log are adequate clay indicators, and in this case behave similarly so that the gas effect can be "stripped out" of the neutron response.

Figure 5 is a crossplot of $(V_{cl})_{gr}$ vs. $(V_{cl})_{dn}$ for the same intervals as the trace plots of Figures 3 and 4. The correlation coefficient is very strong - .920. The correlation of gamma ray vs. neutron is also strong - .797. The better correlation of $(V_{cl})_{gr}$ vs. $(V_{cl})_{dn}$ says that there must be something intrinsically good about including both the density and neutron logs in the clay model - as opposed to using the neutron log alone. The crossplot gives the same value for V_{cl} at .60, which is the clay constant. The low end does not give perfect correlation when calibrated properly because of the gas effect in uninvaded gas sands.

APPLICATION OF THE NEW MODEL TO CALCULATE POROSITY

Equations 6 and 3 are used to compute gas corrected porosity for the core-log crossplot example used earlier. These results are crossplotted with core porosity in Figure 6. There is good agreement (see Figure for statistics) between calculated porosity and core porosity - thus variable unflushed gas effect has been effectively quantified by equation 6. The results are much better than using density data alone (Figure 1). The excellent correlation of both plots are due to exceptional data quality.²

Figure 7, track 1, is a trace plot of calculated porosity and core porosity for the CER MWX-1 well. Again the agreement is excellent, although in this case most of the sands have been partially flushed. In comparison, the porosity interpreted by averaging the density and neutron logs gives a mean value which is 1.5 p.u. higher than core porosity. This is due to clay affecting the neutron log more than the density log.

APPLICATION OF THE NEW MODEL TO INTERPRET GAS
SATURATION IN UNINVADED SANDSTONES

Equation 6 is used to calculate S_{dn} - the water saturation of the zone investigated by the density and neutron tools. This computation is presented in trace plots for the CER MWX-1 example (Figure 7 and Figure 8). Comparison of the S_{dn} with conventionally calculated saturation (total shale equation) demonstrates that the new model gives reasonable results for S_{dn} .

The Corcoran Sandstones (Figure 8) are essentially unflushed and the Cozzette Sandstones (Figure 7) are partially flushed. This is explained by time lapse differences between penetration and logging and differential pressure differences. The Corcoran was logged in an underbalanced condition, whereas the Cozzette is overbalanced. The resemblance of the two saturation curves in the unflushed formation is remarkable. Dissimilarity in the zone 8194-8200' is thought to be due to a "burned out" oil zone (pyrobitumen or solid hydrocarbons). The interval 7832-7854' is confirmed by core data in an adjacent well as being a pyrobitumen zone.

APPLICATION OF THE NEW MODEL TO INTERPRET R_w

In uninvasion sandstones, R_w can be calculated using a combination of equation 6, equation 3 and resistivity data, in much the same way as R_{wa} is calculated. In this case, however, " S_w " is the saturation that is calculated by equation 6 rather than a constant 1.0 as assumed by the R_{wa} equation. This approach is possible since the calculated " S_w " is independent of R_w and R_t .

The CER MWX-1 well is used as an example to demonstrate the new R_w approach. Figure 9 is a trace plot of calculated R_w and R_{wa} curves. The technique involves interpreting the R_w in relatively uninvasion sands. Figures 7 and 8 are used in conjunction to determine the more uninvasion points of the plot. The " R_w uninvasion ss (shaly sand)" curve in track 2 is a foot-by-foot solution for R_w using a conventional shaly sand S_w equation (total shale equation). The saturation input into this equation is S_{dn} . R_w in this case is interpreted to be .12 at T_{fm} . This is in agreement with the resistivity of formation water samples taken from the Cozzette in this and adjacent wells. R_{wa} and R_w using the Archie equation are presented for comparison.

In the described manner, an R_w profile was constructed for the entire 4000' Mesaverde Group interval of the CER MWX-1 well (Figure 10). It is possible to interpret depositional environments and basin hydrodynamics from this plot. For example, the paludal interval (coaly, swampy) has generally fresher formation water. It is hypothesized by Law et al, that the fresher waters of this interval are resultant from the coalification process, i.e., water byproduct dilutes the "connate water."¹⁰

The fresher waters above 5000' are thought to be related to downdip incursion of meteoric water. It should be noted that no other log analysis technique is successful for the interpretation of R_w in this interval.¹

APPLICATION OF THE NEW MODEL TO INTERPRET PERMEABLE ZONES

When the S_{dn} curve is compared to conventional S_w (Figures 7 and 8) it is possible to interpret which zones are invaded. When adequate time and differential pressure exists, filtrate invasion is expected to occur. In such intervals (Figure 7) the saturation curves tend to swing in opposite directions. Intervals capable of being invaded are interpreted to have a matrix permeability capable of producing gas. Uninvaded zones are thought to be too tight for production, even if fractured.

S_{dn} subtracted from conventional S_w (ΔS_w) is sometimes a quantitative permeability indicator. Crossplots of ΔS_w vs. core permeability generally have correlation coefficients of .2 to .4. Interpretation of producibility from invasion profile inferences must be strongly tempered with considerations of time and differential pressure. The Corcoran sands of MWX-1 (Figure 8) are uninvaded for reasons already discussed. Kukul et al (1983) pointed out that producibility is most reliably predicted from the water saturation of such zones.¹

3 intervals in the MWX-1 well have been production tested as follows:

- | | | |
|-------------------|--------------|-----------|
| 1. Lower Corcoran | 8194 - 8230, | 400 MCFD |
| 2. Lower Cozzette | 7940 - 7956 | 200 MCFD |
| 3. Upper Cozzette | 7830 - 7894, | 1000 MCFD |

All flow rates are natural flow following a small breakdown. The formations appear to be naturally fractured.

APPLICATION OF THE NEW MODEL TO GENERATE SYNTHETIC (IN-SITU) DENSITY AND NEUTRON LOGS

Finally for "management types" and for people who enjoy looking at density-neutron crossover, a synthetic log may be generated which plots the density and neutron curves as they would theoretically appear if the formation is totally uninvaded. Figure 11 is an example of generally invaded sands and Figure 12 shows the uninvaded case. A plot of uncorrected density and neutron curves are presented for comparison. Cross sections of these synthetic logs provide better well-to-well comparisons and are therefore of interest to the development geologist.

The computed shaly sand water saturation and the response equations (equations 1 and 2) are used for constructing these plots.

CONCLUSIONS

The "Kukal equation or approach" (equation 6) is shown to be an effective and practical method to compensate for variable unflushed gas saturation in the porosity analysis of TGS sequences. The equation (equation 9) may also be useful to compute clay volume in conventional reservoirs. A new clay volume equation from the gamma ray emphasizes the definition of "clay" as opposed to "shale."

Applications of the new technique are numerous and result in improved analysis of R_w , S_w , and permeability in TGS. The new approach promises to be a powerful new system for geologic studies and formation evaluation.

ACKNOWLEDGEMENT

This research was funded by the U.S. Department of Energy. Thanks are due to R.E. Hill and K.E. Simons with CER who have provided technical support, particularly with the computer work.

REFERENCES

1. Kukal, G.C., Biddison, C.L., Hill, R.E., Monson, E.R., and Simons, K.E.: "Critical Problems Hindering Accurate Log Interpretation of Tight Gas Sand Reservoirs," SPE 11620, Proceedings of the 1983 SPE/DOE Symposium on Low Permeability Gas Reservoirs, March 1983.
2. Kukal, G.C.: "Determination of Fluid Corrected Porosity in Tight Gas Sands and in Formations Exhibiting Shallow Invasion Profiles," SPE 9856, Proceedings of the 1981 SPE/DOE Symposium on Low Permeability Gas Reservoirs, May 1981.
3. Patchett, J.G., and Coalson, E.B.: "The Determination of Porosity in Sandstone and Shaly Sandstone Part Two, Effects of Complex Mineralogy and Hydrocarbons," Transactions of the SPWLA Twenty-Third Annual Logging Symposium, July 1982.
4. Sattler, A.R.: "The Multi-Well Experiment Core Program," SPE 11763, Proceedings of the 1983 SPE/DOE Symposium on Low Permeability Gas Reservoirs, March 1983.
5. Kukal, G.C.: "A Systematic Approach for the Log Analysis of Tight Gas Sands," SPE 11857, Proceedings of the 1983 Rocky Mountain Regional SPE Meeting, May 1983.
6. Sherman, H., and Locke, S.: "Effect of Porosity on Depth of Investigation of Neutron and Density Sondes," SPE 5510, 1975 Fall Meeting of SPE, September 1975.

7. Thomas, R.D., and Ward, D.C.: "Effect of Overburden Pressure and Water Saturation on Gas Permeability of Tight Gas Sandstone Cores," JPT (February 1972) pp. 120-124.
8. Segesman, F., and Liu, O., "The Excavation Effect," Paper N, SPWLA Trans., May 1971.
9. Kukal, G.C. and Hill, R.E.: "Log Analysis in Low Permeability Gas Sand Sequences - Matrix Parameter Refinement," In preparation for The Log Analyst, July-August, 1983.
10. Law, B.E., Hatch, J.R., Kukal, G.C., and Keighin, C.W.: "Geologic Implications of Coal Dewatering: A Hypothesis," Proceedings of AAPG Annual Meeting, April 1983.

ABOUT THE AUTHOR

GERALD KUKAL is Manager of CER's Formation Evaluation Department. He joined CER Corp., Las Vegas in 1977 and spends most of his time developing new log interpretation techniques, especially in the tight gas sands area. Previously, Kukal spent four years with Dresser Atlas. He also has six years' experience teaching geology. He received his BS in 1967 from Southwest Missouri University and MS in 1973 from Purdue University. He has presented technical papers to SPWLA, CWLS, SPE, AAPG, and RMAG.



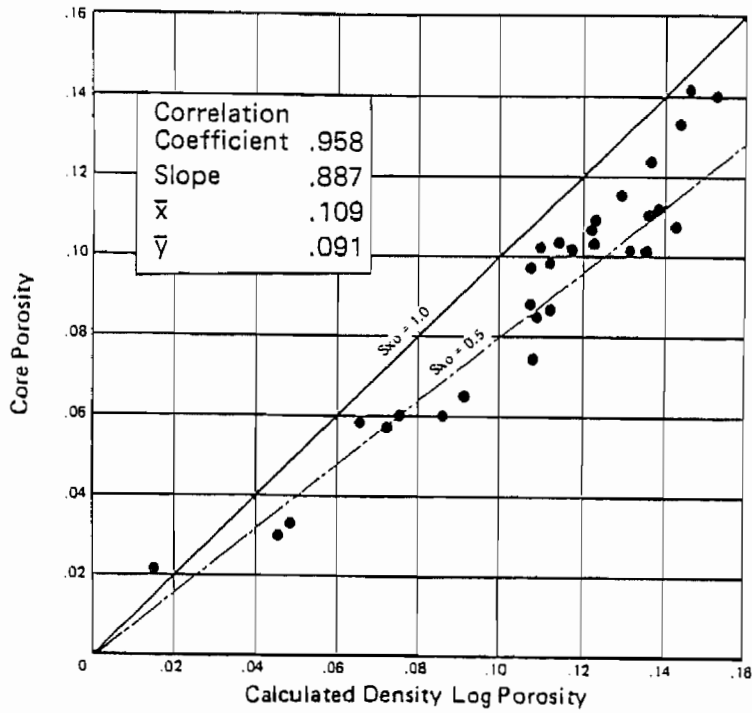


Figure 1 Log-Core Correlation, 4 Wells Western Wyoming, 30 Averaged Zones

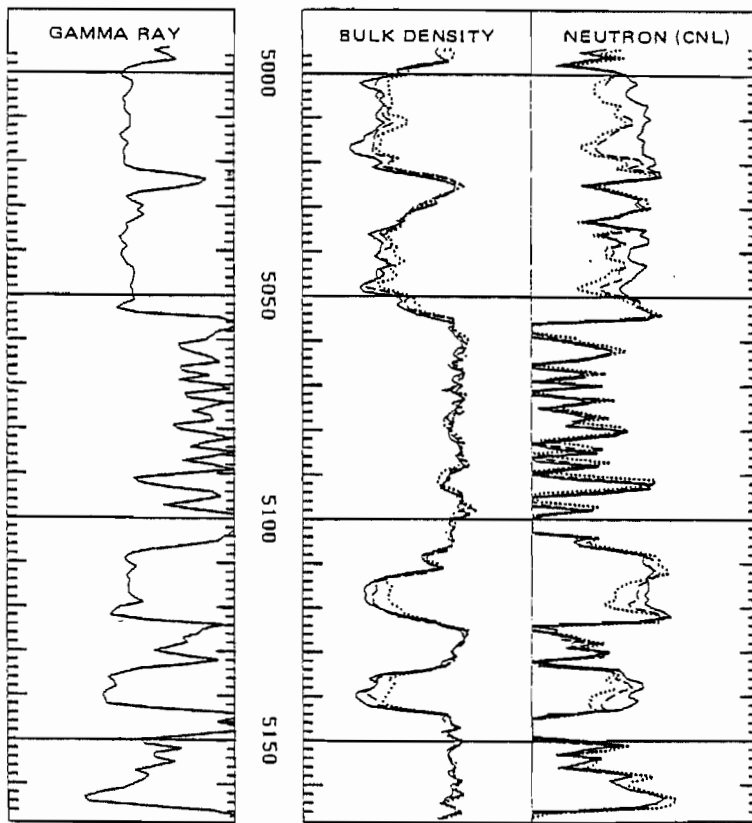


Figure 2 Multiple Log Runs Through TGS Interval Showing Progressive Invasion, CER MWX-2

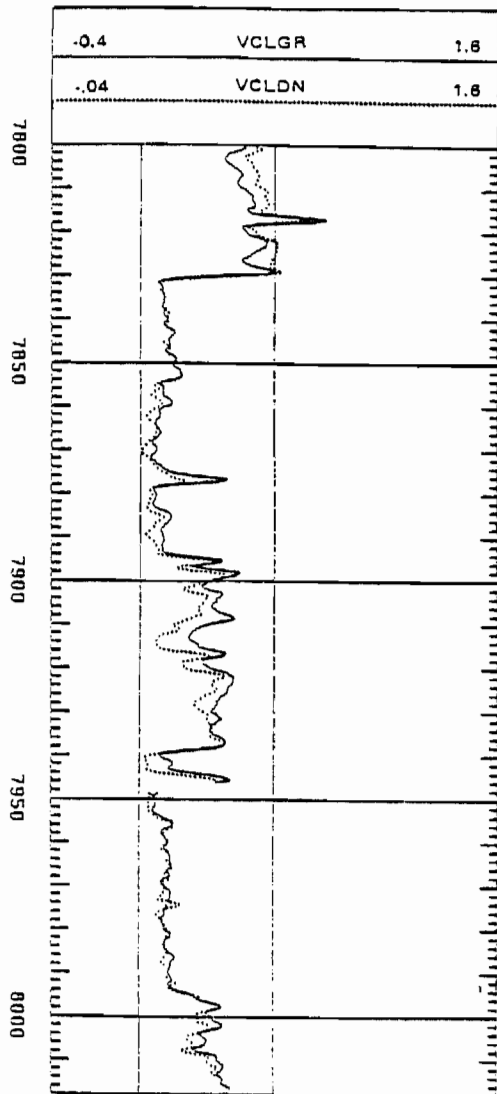


Figure 3 Trace Plot of Equations 7 (VCLGR) and 9 (VCLDN), CER MWX-1 Well, Cozzette Sands

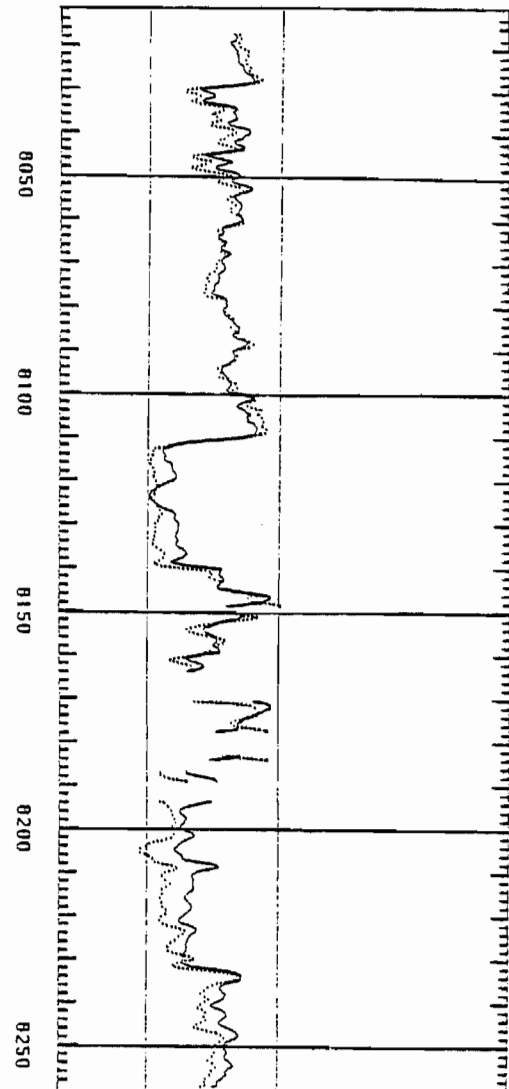


Figure 4 Trace Plot of Equations 7 (VCLDN) and 9 (VCLGR), CER MWX-1 Well, Corcoran Sands

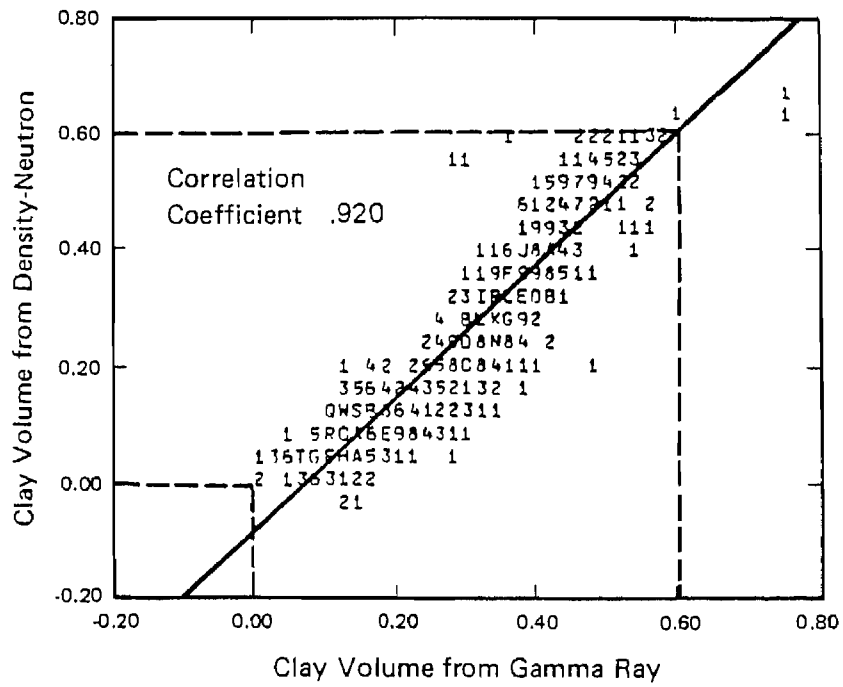


Figure 5 Crossplot Showing Adequate Refinement of Clay/ Matrix Parameters

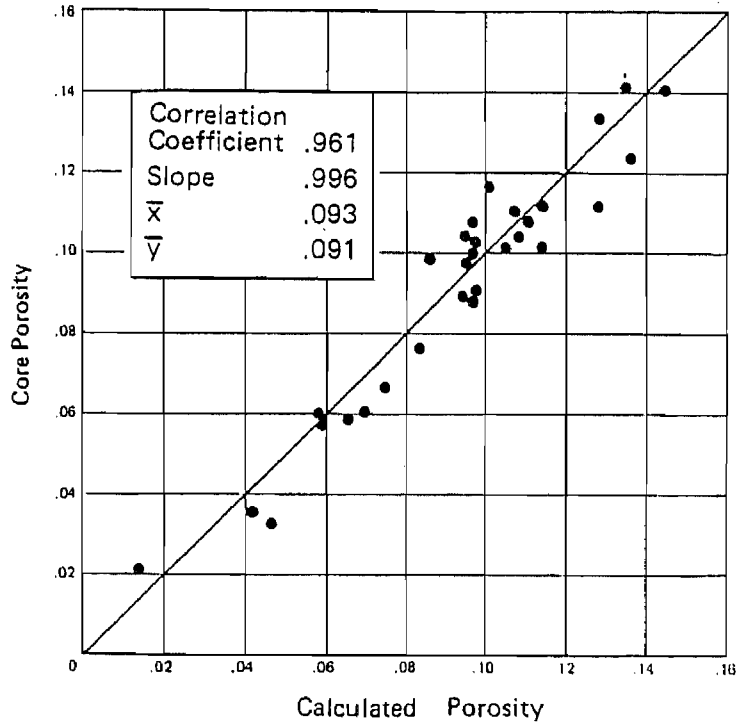


Figure 6 Model Results Vs. Core Porosity - Compare to Figure 1

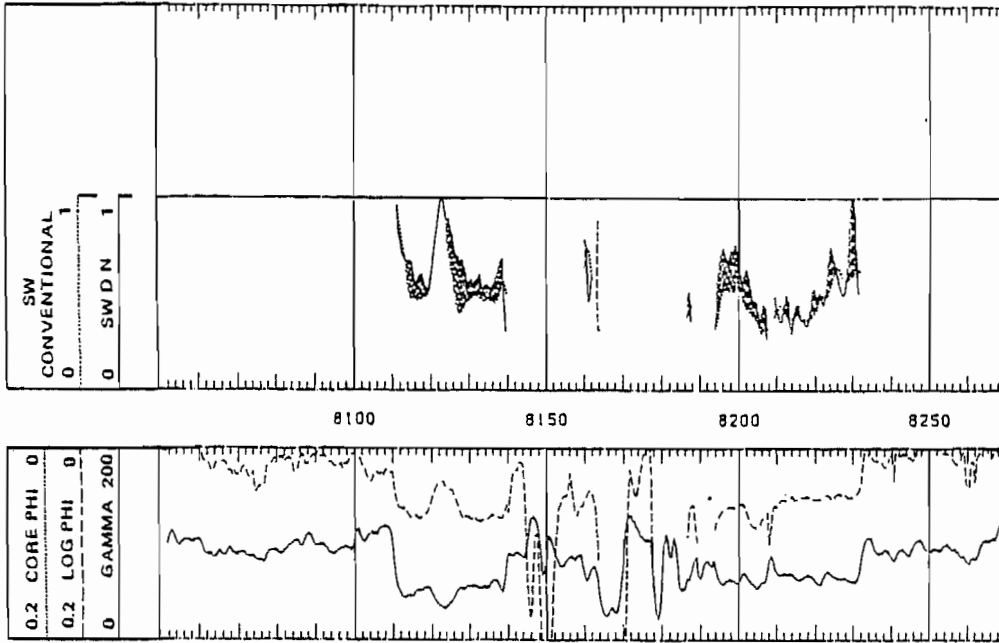


Figure 8 Output of Model Results, CER MWX-1, Corcoran Sands

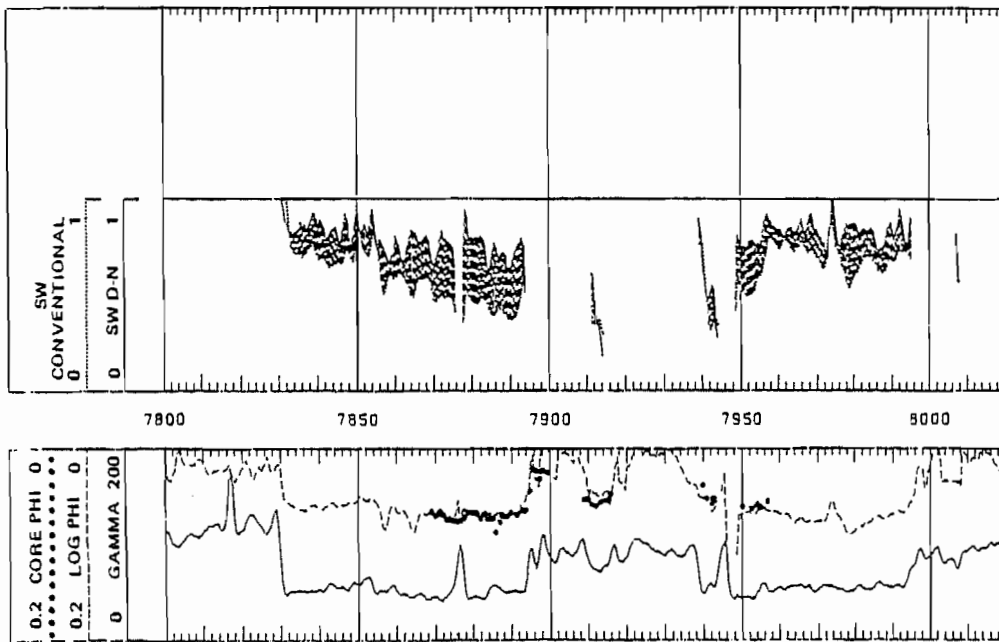


Figure 7 Output of Model Results, CER MWX-1, Cozette Sands

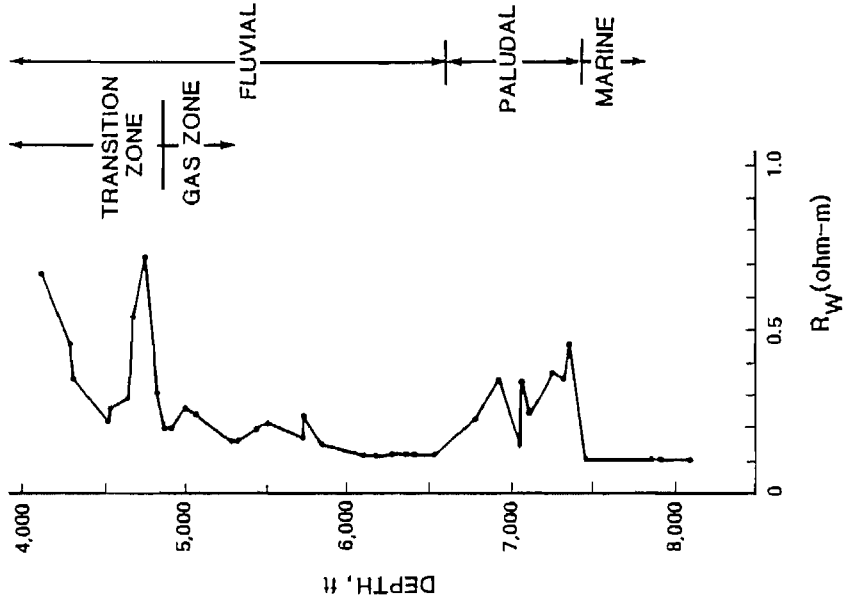


Figure 10 R_w Profile - Interpretation of R_w for Mesaverde Interval, CER MWX-1

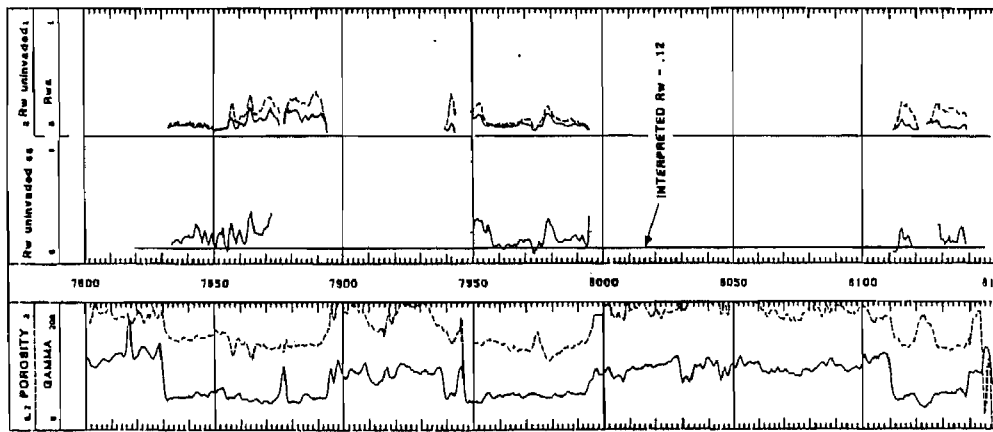


Figure 9 Raw Plot - Raw Calculations, CER MWX-1

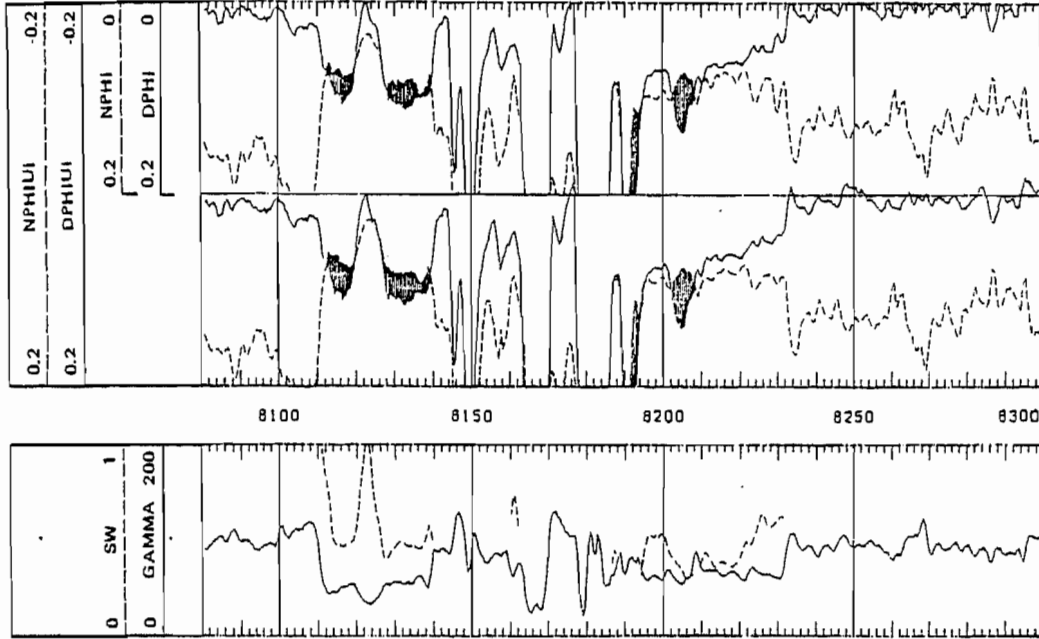


Figure 12 "In Situ Log" CER MWX-1 Corcoran Sands

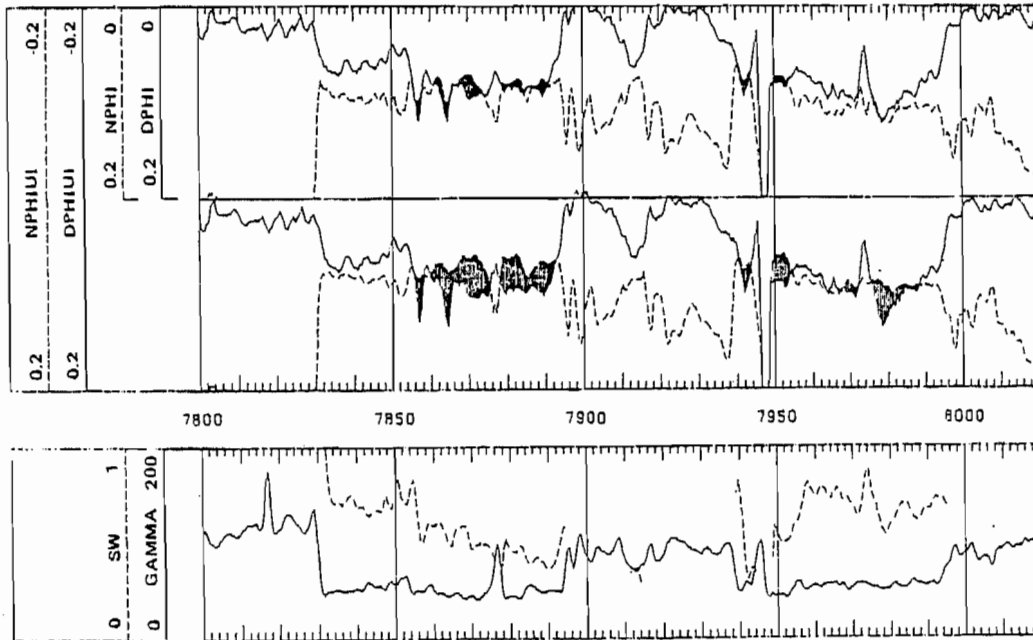


Figure 11 "In Situ Log" CER MWX-1 Cozzette Sands